Water Resources Research

Supporting Information for

Flushing the Lake Littoral Region: the Interaction of Differential Cooling and Mild Winds

Cintia L. Ramón,[1,2*], Hugo N. Ulloa[3,4], Tomy Doda[1,3], and Damien Bouffard[1]

[1] Department of Surface Waters – Research and Management, Eawag (Swiss Federal Institute of Aquatic Science and Technology), Kastanienbaum, Switzerland.

[2]Water Research Institute and Department of Civil Engineering, University of Granada, Granada, Spain.

[3]Physics of Aquatic Systems Laboratory, EPFL (École Polytechnique Fédérale de Lausanne), Lausanne, Switzerland.

[4]Department of Earth and Environmental Science, University of Pennsylvania, Philadelphia, USA

Contents of this file

Introduction

This Supporting Information includes figures, Table S1 and Text S1. Figure S1 shows the modeled unit-width discharges in the downwind littoral region for W-runs in Table 1, where the lake was only forced with a surface wind stress. It also shows the fit of the modeled discharges to Eq. 7 (scaling for wind-driven unit-width discharges). Figure S2 displays the 3D Smagorinsky viscosities within the SML for runs 0-6 and W-runs in Table 1. Figure S3 compares the horizontal Richardson number Ri_x (Eq. 9) with χ_{MO} (Eq. 2). Text S1 and Figures S4 to S6 analyze the sensitivity of q_c to MITgcm input parameters.

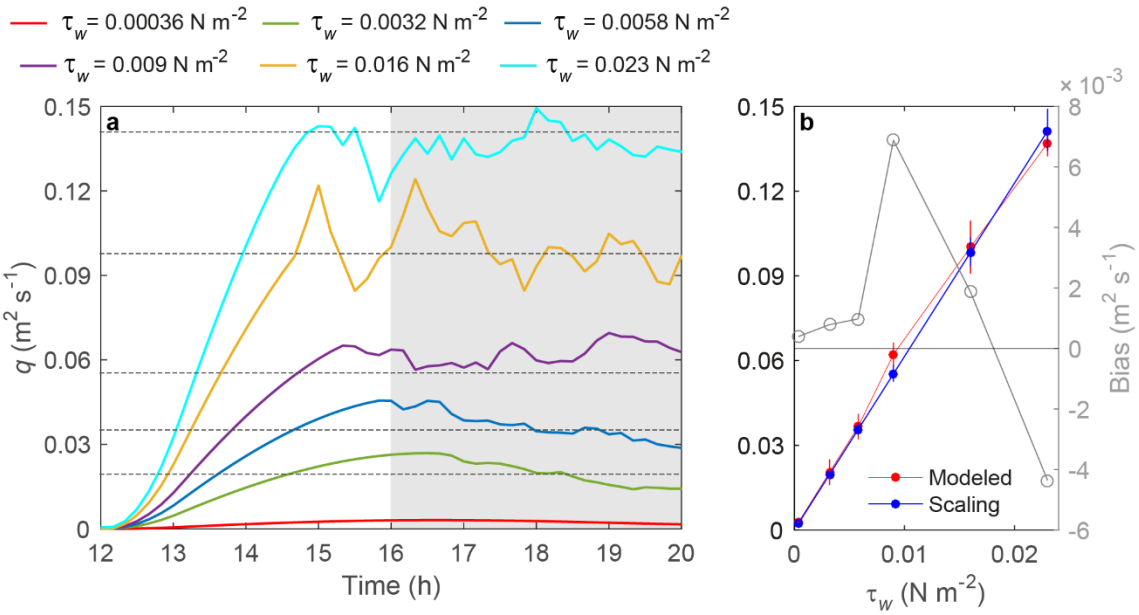

Figure S1. Scaling for wind-driven unit-width discharges. (a) Time series of offshore modeled flows in the downwind side (profile D) for the W-runs in Table 1, and (b) time-averaged modeled unit-width discharges, best-fit scaling (Eq. 7), and bias (= $q_m - q_w$). The period for time averaging (gray-shaded area in (a)) was chosen from 16 h (≈ one-half of the internal wave period from the start of the forcing) until ≈ 20 h when the flow remained quasi-steady. Dotted lines in (a) show the predicted flows using Eq. 7. Vertical lines in the modeled and scaled values in (b) show ± one standard deviation and 95% confidence interval, respectively. Best fit (R^2 = 0.993) was achieved for v_z = 6.0 ± 0.4 × 10^{-4} m^2 s^{-1}.

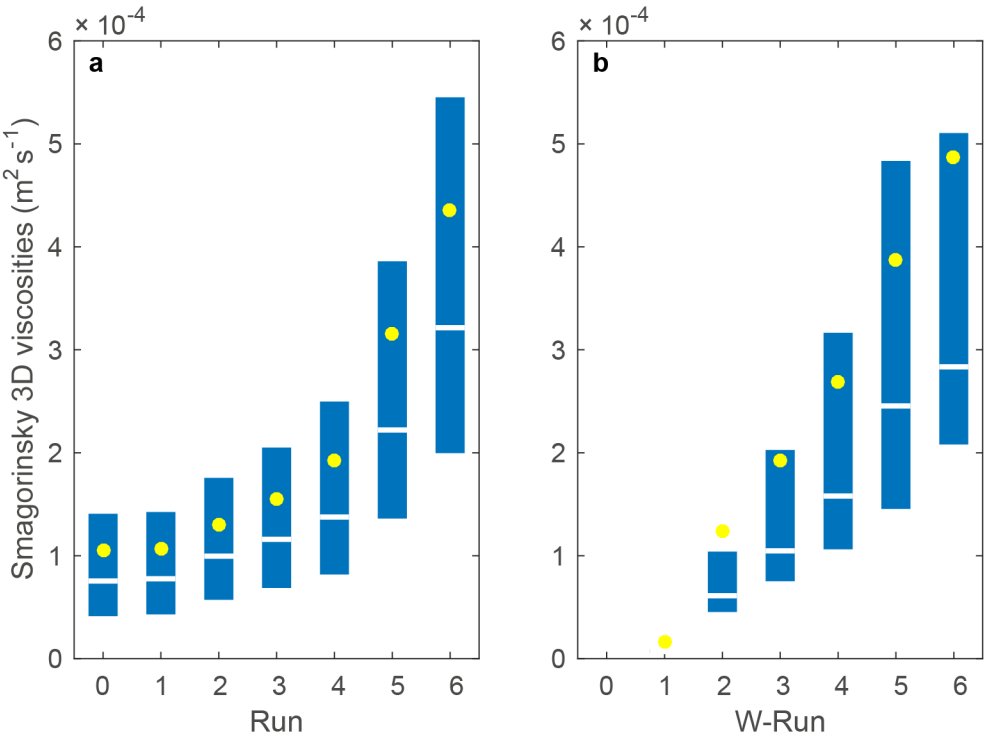

Figure S2. Modeled 3D Smagorinsky viscosities within the SML and during the quasi-steady state ($t > t_{ss\text{-}wind}$). Results for (a) runs 0-6 and (b) W-runs 1-6 in Table 1. Blue rectangles show the interquartile range; white lines, median values; and yellow dots, mean values.

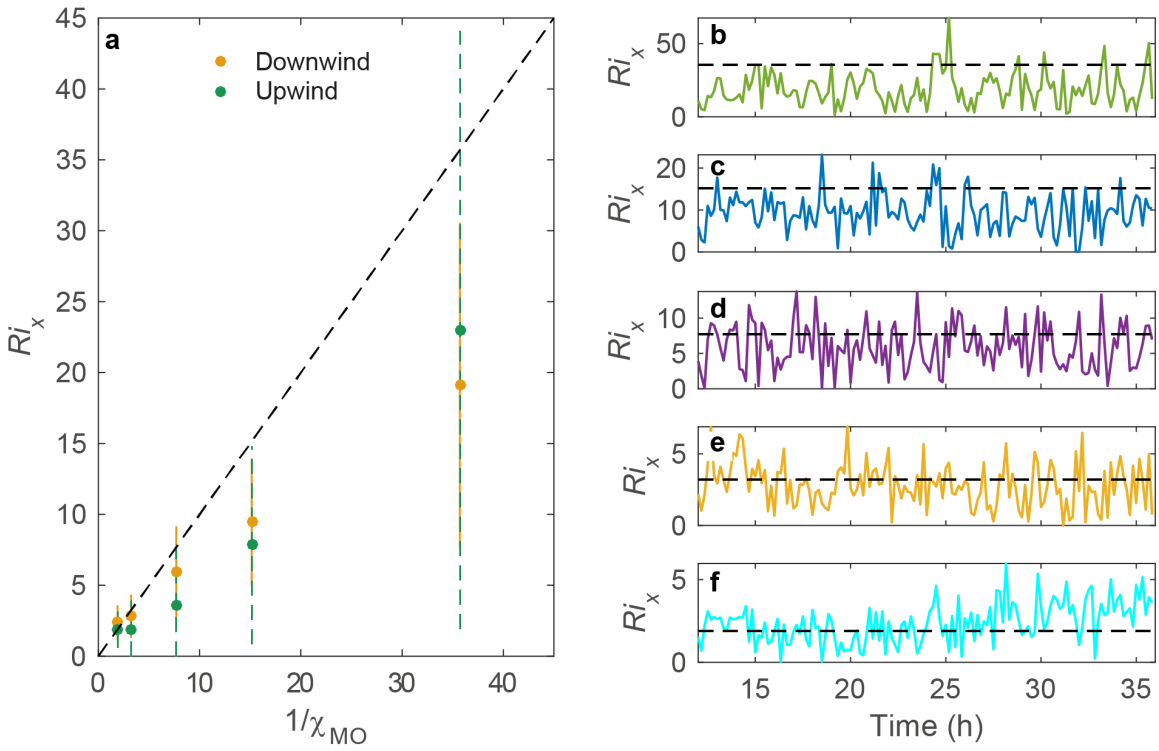

Figure S3. Relationship between Ri_x (Eq. 9) and χ_{MO} (Eq. 2). (a) Time-averaged horizontal Richardson number Ri_x versus χ_{MO}^{-1} for runs 2 to 6 in Table 1. Vertical lines show ± one standard deviation of Ri_x and the black dashed line the 1:1 relationship. (b-f) Time series of Ri_x in the downwind region for (b) run 2 (χ_{MO} = 0.028), (c) run 3 (χ_{MO} = 0.066), (d) run 4 (χ_{MO} = 0.13), (e) run 5 (χ_{MO} = 0.31) and (f) run 6 (χ_{MO} = 0.53). Black dashed lines in b-f show χ_{MO}^{-1}. Ri_x was calculated with the average horizontal density gradient within the littoral region and the littoral region's average depth (h_{lit}).

Text S1. Notes on the sensitivity of q_c to MITgcm input parameters.

Ulloa et al. (2022) performed 2D Spectral LES simulations to examine the development of thermal siphons driven by a uniform loss of heat at the air-water interface in sloping, stratified basins. The length of their 2D basin was 800 m in the *x*-direction and expanded only 1-m in the y-direction. The basin topography in the *x*-direction was characterized by two littoral regions at the two edges of the lake (Fig. S4). Each littoral region is composed of a flat zone of uniform depth h_p = 1 m and length l_p, connected to a sloping region of length l_s that progressively increases in depth from h_p to h_{SML} = 4.5 m (Fig. S4-top). In their Exp. 1, $L_{SML} = l_p + l_s \approx 238$ m and the average longitudinal slope in the sloping region $S_s = (h_{SML} - h_p)\, l_s^{-1}$ is ≈ 0.03. The interior region has a maximum depth *H* of 7 m. The initial thermal stratification followed a smooth function of the form:

$$T(x,z) = T_b + \frac{\Delta T}{2}\left\{1 + tanh\left(\frac{z-(H-h_T)}{\delta}\right)\right\}$$

Where T_b (= 8.5°C) is the bottom temperature in the interior basin, $T_s = T_b + \Delta T$ (= 14 °C) is the temperature at the water surface, h_T (= 5 m) is the depth of the thermocline and δ (= 0.5 m) is half the metalimnion thickness. The lake surface boundary was subject to a uniform heat loss rate Q_0, which led to a destabilizing buoyancy flux $B_0 = 7\times10^{-9}$ W kg^{-1}. Q_0 was constant over time and the simulated period was 24h. Note that B_0 in their experiments is one order of magnitude lower than in this study.

We reproduced their LES Exp. 1 with MITgcm as a benchmark test to analyze the sensitivity of the results to the selected model parameters, with an especial focus on background horizontal viscosities. We kept the same grid resolution and model configuration as explained in the main text (Section 2.2). Water density was calculated with the modified nonlinear UNESCO equation of state (Jackett & Mcdougall, 1995) as in Ulloa et al. (2022). We used the cross-shore evolution of the thermal siphon discharges in the littoral region $q_{TS}(x)$ as the variable of calibration. The selected period for model calibration was the quasi-steady regime, which for Exp. 1 develops at t > 18h (details in Ulloa et al., 2022). For calibration purposes, horizontal background viscosities $v_{h\text{-}bck}$ were allowed to vary from O(10^{-6}) m^2 s^{-1} to (10^{-3}) m^2 s^{-1} and the 3D Smagorinsky constant from 5×10^{-5} to 5×10^{-4}. Tests were also conducted where we varied the magnitude of the background horizontal and vertical diffusivities, $K_{h\text{-}bck}$ and $K_{z\text{-}bck}$ (Table S1). The best fit was achieved for horizontal viscosities of 1×10^{-4} m^2 s^{-1}, 3D Smagorinsky constant = 1×10^{-4} (Fig. S4), $K_{h\text{-}bck} = 10^{-5}$ m^2 s^{-1} and $K_{z\text{-}bck} = 1.4\times10^{-7}$ m^2 s^{-1} (run 9 in Table S1), with a Root Mean Squared Error RMSE between LES and MITgcm q_{TS} of 0.0016 m^2 s^{-1}, which represent 13% of maximum LES unit-width discharges in the littoral region. MITgcm correctly reproduced the temperature T_{TS} (RMSE = 0.007°C) and thickness h_{TS} (RMSE = 0.2 m) of the bottom offshore-flowing layer, as well as the density difference between the top and bottom layers, with an RMSE for the reduced gravity $g' = g\Delta\rho/\rho_{TS}$ of O(10^{-5}) m s^{-1} (Fig. S4).

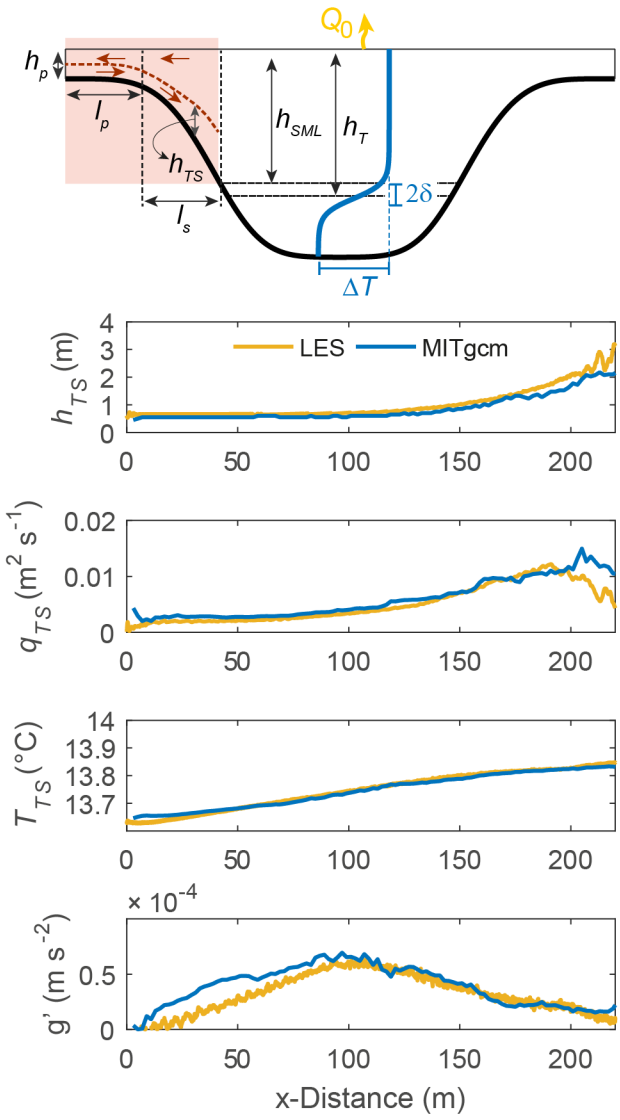

Table S1: Sensitivity of q_c to MITgcm input parameters. Model runs and calibration parameters.

run	$\nu_{h\text{-}bck}$	Smag3D	$K_{h\text{-}bck}$ (m^2 s^{-1})	$K_{z\text{-}bck}$ (m^2 s^{-1})
1	1×10^{-6}	1×10^{-4}	1×10^{-5}	1.4×10^{-7}
2	1×10^{-5}	1×10^{-4}	1×10^{-5}	1.4×10^{-7}

3	1×10^{-5}	5×10^{-4}	1×10^{-5}	1.4×10^{-7}
4	1×10^{-5}	1×10^{-4}	1×10^{-6}	1.4×10^{-7}
5	1×10^{-5}	1×10^{-4}	1×10^{-5}	1×10^{-5}
6	1×10^{-4}	1×10^{-4}	1×10^{-5}	1×10^{-6}
7	5×10^{-5}	5×10^{-5}	1×10^{-5}	1.4×10^{-7}
8	5×10^{-5}	1×10^{-4}	1×10^{-5}	1.4×10^{-7}
9	1×10^{-4}	1×10^{-4}	1×10^{-5}	1.4×10^{-7}
10	1×10^{-4}	1×10^{-4}	1×10^{-4}	1.4×10^{-7}
11	1×10^{-4}	1×10^{-4}	1×10^{-6}	1.4×10^{-7}
12	1×10^{-4}	1×10^{-4}	1×10^{-5}	1×10^{-6}
13	1×10^{-4}	1×10^{-4}	1×10^{-5}	1×10^{-5}
14	1×10^{-4}	5×10^{-4}	1×10^{-5}	1.4×10^{-7}
15	5×10^{-4}	1×10^{-4}	1×10^{-5}	1.4×10^{-7}
16	5×10^{-4}	5×10^{-4}	1×10^{-5}	1.4×10^{-7}
17	1×10^{-3}	1×10^{-4}	1×10^{-5}	1.4×10^{-7}
18	1×10^{-3}	1×10^{-4}	1×10^{-3}	1.4×10^{-7}
19	4×10^{-3}	1×10^{-4}	1×10^{-5}	1×10^{-5}
20	4×10^{-3}	5×10^{-4}	1×10^{-5}	1.4×10^{-7}
21*	1×10^{-5}	1×10^{-4}	1×10^{-5}	1.4×10^{-7}
22*	1×10^{-3}	1×10^{-4}	1×10^{-5}	1.4×10^{-7}
23*	4×10^{-3}	1×10^{-4}	1×10^{-5}	1.4×10^{-7}

*For these runs B_0 was increased to match the value used in this study, i.e., $B_0 = 5.2\times10^{-8}$ W kg^{-1}

Several combinations of input parameters resulted in modeled unit-width discharges q at the offshore end of the littoral region within the range of variability (± one standard deviation) of the LES modeled unit-width discharges (gray shaded area in Fig. S5). In general, MITgcm q increased with increasing values of $v_{h\text{-}bck}$ and decreased with increasing values of $K_{z\text{-}bck}$. For the tested $v_{h\text{-}bck}$ range, q reached its maximum value for $v_{h\text{-}bck} = 1 \times 10^{-3}$ m^2 s^{-1} with mean values that almost double mean LES data (see run 17 in Fig. S4). For the highest $v_{h\text{-}bck}$ (= 4×10^{-3} m^2 s^{-1}) increasing $K_{z\text{-}bck}$ from 1.4×10^{-7} to 1×10^{-5} m^2 s^{-1} improved the predictability of q (run 19) but led to unrealistic vertical mixing in the main basin, that resulted in the progressive shallowing instead of deepening of the thermocline in the interior basin.

The sensitivity of q to the background $v_{h\text{-}bck}$ became however less pronounced as B_0 increased one order of magnitude from $B_0 = 7 \times 10^{-9}$ W kg^{-1} as in Ulloa et al. (2022) to $B_0 = 5.2 \times 10^{-8}$ W kg^{-1} as used in this study. Increasing horizontal viscosities from O(10^{-5}) to O(10^{-3}) m^2 s^{-1} resulted in less than 20% variability in the modeled q (see results from runs 21-23 in Fig. S5). Similarly, using the 3D trapezoidal bathymetry in Fig. 1 (main text) and $B_0 = 5.2 \times 10^{-8}$ W kg^{-1} resulted in less than 35% variability in the predicted offshore discharges at U and D locations for $\chi_{MO} = 0$ and a horizontal viscosity range O(10^{-4}-10^{-3}) m^2 s^{-1} (Fig. S6).

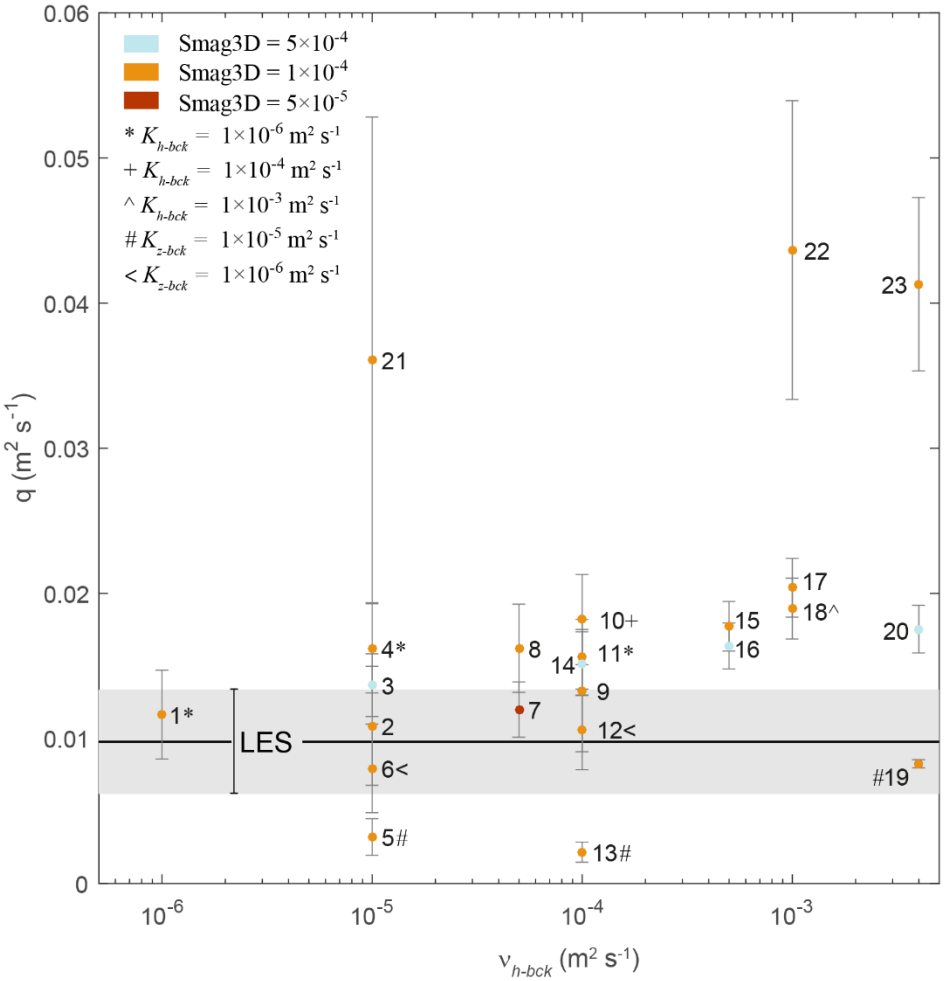

Figure S5. Modeled unit-width discharges at the offshore end of the littoral region for different background horizontal viscosities $\nu_{h\text{-}bck}$, 3D Smagorinsky constant Smag3D and vertical and horizontal background diffusivities $K_{z\text{-}bck}$ and $K_{h\text{-}bck}$ (runs 1-23 in Table S1). The color of a dot indicates the value of Smag3D. Symbols beside a run number indicate that $K_{z\text{-}bck}$ or $K_{h\text{-}bck}$ differ from $K_{h\text{-}bck}$ = 10^{-5} m^2 s^{-1} and $K_{z\text{-}bck}$ = 1.4×10^{-7} m^2 s^{-1}. The lake basin and forcing conditions are the same as in Exp. 1 in Ulloa et al. (2022), except for runs 21-23 where B_0 was increased to 5.2×10^{-8} W kg^{-1}. Results are presented for Regime 3 (quasi-steady period). Dots represent mean values for each MITgcm run and the vertical lines indicate ± one standard deviation. Mean LES results are represented by a black horizontal line and the gray shaded area represents ± one standard deviation.

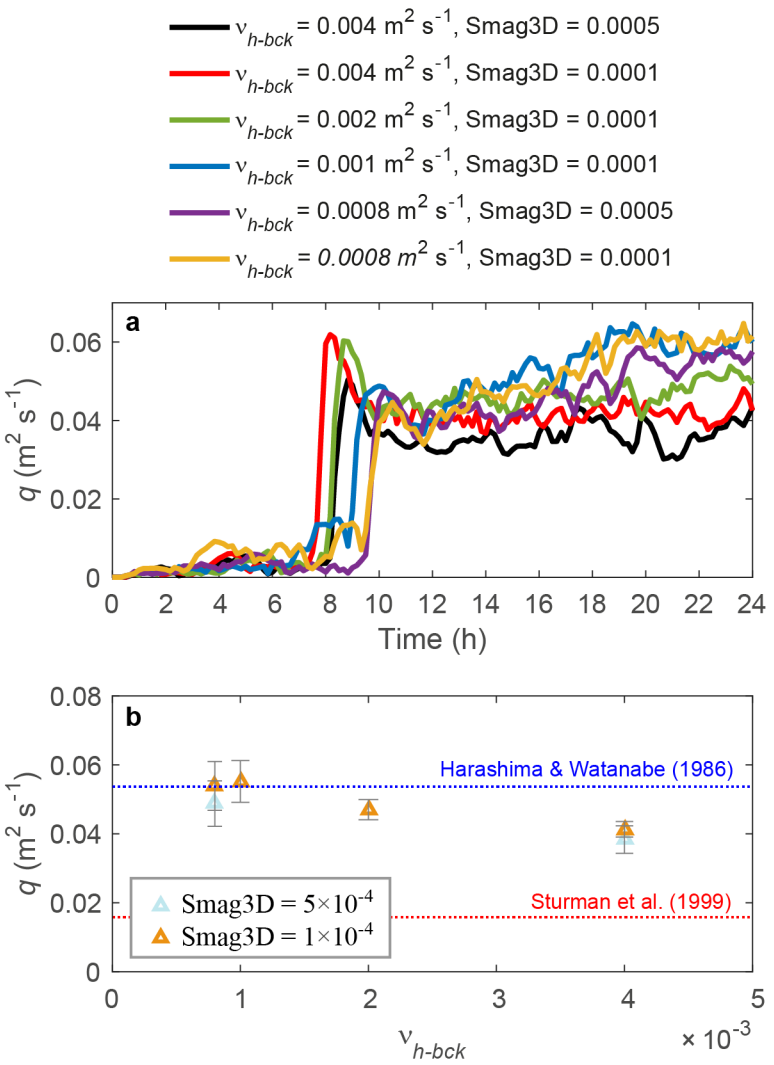

Figure S6. Sensitivity of offshore unit-width discharges to the selected background viscosities for χ_{MO} = 0. Bathymetry and forcing conditions as in Section 2.3 in the main text. (**a**) Evolution in time of the modeled cross-shore unit width discharges at the offshore end of the littoral region (U profile in Fig. 1a). (**b**) Mean flow ± one standard deviation at this location during the quasi-steady-state period. The Horizontal dashed blue line shows the theoretical discharges calculated with Eq. 1 and the empirical relationship for constant *a* from Harashima & Watanabe (1986). The horizontal dashed red line shows the scaling $q_c = 0.24\ B_0^{1/3}\ (L_{SML}S/(1+S))^{4/3}$ proposed for wedge-shaped littoral regions by Sturman et al. (1999).